Generalized Fowler-Nordheim Theory of Field Emission of Carbon Nanotubes

Shi-Dong Liang* and Lu Chen†

State Key Laboratory of Optoelectronic Material and Technology and School of Physics and Engineering, Sun Yat-Sen University, Guangzhou, 510275, People's Republic of China

(Received 26 September 2007; published 10 July 2008)

Based on the low-energy band structure of carbon nanotubes (CNs), we develop a generalized Fowler-Nordheim theory of the CN field emission, in which the behavior of the current-voltage (I-V) characteristics depends on the electric field and the diameter of the CNs. This formalism reveals the key differences of field emission between conventional bulk metallic emitters and low-dimensional emitters and gives a clear physical understanding of the non-Fowler-Nordheim feature of the I-V characteristics of the CN field emission.

DOI: 10.1103/PhysRevLett.101.027602 PACS numbers: 79.70.+q, 73.63.Fg

Cold electron sources based on field emission promise a potential application in high monochromatic electron-beam production and in new types of displays [1]. Experimental investigations show strong evidence that carbon nanotubes (CNs) can act as point electron sources in high-resolution electron-beam instruments [2]. The reduced brightness of individual multiwall carbon nanotubes is more than 10 times sharper than that of the Schottky emitter and the cold field-emission gun [2]. The early theory of field emission was developed based on the free-electron model, which was long successful [3]. However, the rapid progress of nanotechnology allows the synthesis of many low-dimensional and nanoscale materials. This development provides us with many new choices for field-emission materials [4]. CNs exhibit excellent field-emission features, a low threshold field, and a high current density [1]. Nevertheless, it is found experimentally that the current-voltage (I-V) characteristic deviates from the Fowler-Nordheim (FN) type of behavior at the high current density [1]. This phenomenon is usually attributed to the space charge effect [5]. However, experimental results suggest that the space charge effect should not dominate this deviation phenomena from the FN behavior [1]. Another possible explanation from first-principles calculations is the field penetration effect [6]. So far, this non-FN behavior of the CN field emission is not clearly understood [1]. It should be noted that the FN theory of field emission neglects the effect of the energy band structure of the emitter [3]. Since the CN is a quasi-one-dimensional object, its energy band structure plays an important role in the electronic transport and in the field emission [7]. The low-energy band structure of CNs exhibits the Luttinger liquid behavior that has been observed experimentally and attracted much attention [8]. The feature of the CN energy band structure should help us to explain the field-emission characteristics of CNs.

In this Letter, taking into account the low-energy band structure of CNs, we will develop a generalized FN theory of CN field emission. This theory may also be useful in general to understand certain physical properties of low-dimensional systems.

For the field emission of CNs, it is assumed that the electrons in the conduction band of CNs move along the tube layer under the applied field and tunnel through the vacuum potential barrier. The emission current is given by [7,9],

$$j(F,T) = \sum_q \int_{\mathrm{BZ}} N[E_q(k)] D[E_q(k), F] dk, \tag{1}$$

where $N[E_q(k)] = \frac{e}{\pi\hbar}\frac{\partial E_q(k)}{\partial k} f[E_q(k)] > 0$ is the supply function, where $f[E_q(k)]$ is the Fermi-Dirac distribution function. The $D[E_q(k), F]$ in Eq. (1) is the tunneling probability through the vacuum potential barrier. The main features of the vacuum potential barrier for field emission can be approximated by a triangular-shaped barrier $U(x, F) = \phi - eFx$, where $x = 0$ is set at the end of the CN, ϕ is the work function, and F is the local electric field. This simple form of the potential barrier has been valuable to explain some physical features [7,10], such as the chiral effect [7], the quantum size effect [7], and the Aharonov-Bohm phase effect in field emission [7]. The tunneling probability can be expressed approximately as [9]

$$D[E_q(k), F] = \begin{cases} \exp[-b_0 + c_0 E_q(k)] & \text{for } E_q(k) < \phi, \\ 1 & \text{for } E_q(k) > \phi, \end{cases} \tag{2}$$

where $b_0 = \frac{4}{3}\sqrt{2m/\hbar^2}\frac{\phi^{3/2}}{eF}$, $c_0 = 2\sqrt{2m/\hbar^2}\frac{\phi^{1/2}}{eF}$, and $E_q(k)$ is the energy dispersion relation of the CN, which is measured relatively to the Fermi level. The k and q are quantum numbers labeling the wave vector of the electron along the tube and the transversal modes of the tube.

The energy dispersion relation of the single-wall CN (SWCN) can be obtained from that of graphene. In the low-energy approximation, the energy dispersion relation of graphene can be obtained [11]: $E(k) = \pm(\sqrt{3}/2)at|\mathbf{k} - \mathbf{k_F}|$, where a is the lattice constant of the hexagon and t is the electron hopping amplitude. The energy dispersion relation is linear and radially symmetric around the point K. This is a typical characteristic of the Dirac electrons [8].

 © 2008 The American Physical Society

The states near the Fermi level play the main role in field emission.

For SWCNs, the electronic motion in the transversal direction is constrained so that the energy dispersion relation is discrete in the transversal direction. For the metallic SWCNs, one of the discrete lines passes the K point in the first Brillouin zone shown in Fig. 1. The energy dispersion relation around the K point is approximately symmetric, and it can be written for low-energy levels as

$$E_q(k) = q\Delta E_\perp, \tag{3}$$

where $q = 0, \pm 1, \pm 2, \ldots$, labeling the parallel lines in the first Brillouin zone [see Fig. 1(a)], and $\Delta E_\perp \approx (\sqrt{3}/d)at$ is the energy distance between the two parallel lines [11], where d is the diameter of the tube. Using Eqs. (2) and (3) and carrying out the integration and summation in Eq. (1), we can obtain the emission current as [12]

$$j_m(F,T) = \alpha \frac{F}{\phi^{1/2}} e^{-b\phi^{3/2}/F}\left[\frac{\pi c_0 k_B T}{\sin(\pi c_0 k_B T)} + \frac{2e^{-2\gamma\phi^{1/2}/Fd}}{1-e^{-2\gamma\phi^{1/2}/Fd}} - \frac{2e^{-2\eta\gamma\phi^{1/2}/Fd}}{\eta(1-e^{-2\eta\gamma\phi^{1/2}/Fd})}\right], \tag{4}$$

where $\alpha = e^2/2\pi\sqrt{2m} = 7.558\ \mu\mathrm{A}\,(\mathrm{eV})^{-1/2}e(\mathrm{nm})$, $b = \frac{4}{3e}\sqrt{2m/\hbar^2} = 6.83\ \mathrm{eV}^{-3/2}\,\mathrm{V}(\mathrm{nm})^{-1}$, $\gamma = at\sqrt{6m}/\hbar e = 5.988\ (\mathrm{eV})^{1/2}e^{-1}$, and $\eta = \frac{1}{c_0 k_B T} - 1$. We note that for low temperatures $T \leq 300$ K, $c_0 k_B T \ll 1$, the third term in Eq. (4) can be neglected. Hence we can simplify the Eq. (4) to yield

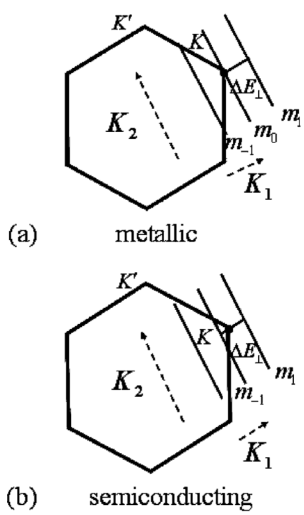

FIG. 1. The first Brillouin zones of SWNT around the K point. For (a) metallic tubes, $q = m_0$ labels the line across the K point. For (b) semiconducting tubes, $q = m_{\pm 1}$ labels the two lines near the K point.

$$j_m(F) = \alpha \frac{F}{\phi^{1/2}} e^{-b\phi^{3/2}/F}\coth\left(\frac{\gamma\phi^{1/2}}{Fd}\right). \tag{5}$$

For semiconducting SWCNs, noting that the parallel lines in the first Brillouin zone do not pass the K point and considering the symmetry of the first Brillouin zone, the energy dispersion relation can be written as $E_q(k) = \pm[(q-\frac{1}{3})\Delta E_\perp + (q-\frac{2}{3})\Delta E_\perp]$, where $q = 1, 2, \ldots$. Using a similar derivation, we can obtain the emission current [12].

$$j_s(F,T) = \alpha \frac{F}{\phi^{1/2}} e^{-b\phi^{3/2}/F}\left[\frac{e^{-2\gamma\phi^{1/2}/3Fd} + e^{-4\gamma\phi^{1/2}/3Fd}}{1-e^{-2\gamma\phi^{1/2}/Fd}} - \frac{e^{-2\eta\gamma\phi^{1/2}/3Fd} + e^{-4\eta\gamma\phi^{1/2}/3Fd}}{\eta(1-e^{-2\eta\gamma\phi^{1/2}/Fd})}\right]. \tag{6}$$

At low temperatures $T \leq 300$ K, the second term in Eq. (6) is negligible, and the emission current becomes

$$j_s(F) = \alpha \frac{F}{\phi^{1/2}} e^{-b\phi^{3/2}/F}\frac{\cosh(\gamma\phi^{1/2}/3Fd)}{\sinh(\gamma\phi^{1/2}/Fd)}. \tag{7}$$

The emission currents in Eqs. (5) and (7) give general formulas of field-emission currents for the metallic and semiconducting SWCNs, respectively, which modify the conventional FN formula of the emission current [3]. Based on the parabolic energy dispersion, the elementary FN equation can be written as [3,13] $j_{\mathrm{FN}}(F) = A\frac{F^2}{\phi}e^{-b\phi^{3/2}/F}$, where $A = 1.541\ \mu\mathrm{A}\,(\mathrm{eV})(\mathrm{V})^{-2}$. In order to compare the formulas of the emission current in Eq. (5) and (7) with the FN-type formula, we distinguish three regions according to different fields and tube diameters. For the cases of small-diameter tubes and low fields (SDLF), $\frac{\gamma\phi^{1/2}}{Fd} \equiv y \gg 1$, $\coth(y) \approx 1$, and in the second-order approximation for the cases of large-diameter tubes and high fields (LDHF), $y \ll 1$, the emission current in Eq. (5) can be expressed as

$$j_m(F) = \begin{cases} \alpha(\frac{F^2 d}{\gamma\phi} + \frac{\gamma}{2d})e^{-b\phi^{3/2}/F} & \text{for } \frac{\gamma\phi^{1/2}}{Fd} < 0.5, \\ \alpha\frac{F}{\phi^{1/2}}e^{-b\phi^{3/2}/F}\coth(\frac{\gamma\phi^{1/2}}{Fd}) & \text{for } 0.5 < \frac{\gamma\phi^{1/2}}{Fd} < 2, \\ \alpha\frac{F}{\phi^{1/2}}e^{-b\phi^{3/2}/F} & \text{for } \frac{\gamma\phi^{1/2}}{Fd} > 2, \end{cases} \tag{8}$$

where we used 0.5 and 2 as an approximation of the dimensionless parameter $\frac{\gamma\phi^{1/2}}{Fd}$ to separate three regions. Similarly, for the semiconducting tubes, we can express the emission current as

$$j_s(F) = \begin{cases} \alpha(\frac{F^2 d}{\gamma\phi} + \frac{\gamma}{18d})e^{-b\phi^{3/2}/F} & \text{for } \frac{\gamma\phi^{1/2}}{Fd} < 0.5, \\ \alpha\frac{F}{\phi^{1/2}}e^{-b\phi^{3/2}/F}\frac{\cosh(\gamma\phi^{1/2}/3Fd)}{\sinh(\gamma\phi^{1/2}/Fd)} & \text{for } 0.5 < \frac{\gamma\phi^{1/2}}{Fd} < 2, \\ \alpha\frac{F}{\phi^{1/2}}e^{-b\phi^{3/2}/F}e^{-2\gamma\phi^{1/2}/3Fd} & \text{for } \frac{\gamma\phi^{1/2}}{Fd} > 2. \end{cases} \tag{9}$$

It can be seen from Eqs. (8) and (9) that the behavior of the I-V characteristic is different in different regions. To compare the I-V behaviors in Eqs. (8) and (9) with the FN-type behavior, we rewrite Eq. (8) in the so-called FN plot form:

$$\ln\left(\frac{j_m(F)}{F^2}\right) = \begin{cases} -\frac{b\phi^{3/2}}{F} + \ln(\frac{\alpha d}{\gamma\phi} + \frac{\alpha\gamma}{2F^2 d}) & \text{for } \frac{\gamma\phi^{1/2}}{Fd} < 0.5, \\ -\frac{b\phi^{3/2}}{F} + \ln(\frac{\alpha}{\phi^{1/2}F}) + \ln\coth(\frac{\gamma\phi^{1/2}}{Fd}) & \text{for } 0.5 < \frac{\gamma\phi^{1/2}}{Fd} < 2, \\ -\frac{b\phi^{3/2}}{F} + \ln(\frac{\alpha}{\phi^{1/2}F}) & \text{for } \frac{\gamma\phi^{1/2}}{Fd} > 2. \end{cases} \quad (10)$$

Similarly, for the semiconducting tubes in Eq. (9), we have

$$\ln\left(\frac{j_s(F)}{F^2}\right) = \begin{cases} -\frac{b\phi^{3/2}}{F} + \ln(\frac{\alpha d}{\gamma\phi} + \frac{\alpha\gamma}{8F^2 d}) & \text{for } \frac{\gamma\phi^{1/2}}{Fd} < 0.5, \\ -\frac{b\phi^{3/2}}{F} + \ln(\frac{\alpha}{\phi^{1/2}F}) + \ln\frac{\cosh(\gamma\phi^{1/2}/3Fd)}{\sinh(\gamma\phi^{1/2}/Fd)} & \text{for } 0.5 < \frac{\gamma\phi^{1/2}}{Fd} < 2, \\ -\frac{b\phi^{3/2}}{F} + \ln(\frac{\alpha}{\phi^{1/2}F}) - \frac{2}{3}\frac{\gamma\phi^{1/2}}{Fd} & \text{for } \frac{\gamma\phi^{1/2}}{Fd} > 2. \end{cases} \quad (11)$$

The first terms in Eqs. (10) and (11) are still of the FN type, but the second and third terms modify the FN-type behavior for different parameter regions. Interestingly, in the SDLF region, the FN plot of the I-V characteristic may be rewritten as $\ln(j_m/F) = -b\phi^{3/2}/F + \ln(\alpha/\phi^{1/2})$ for the metallic tubes, which is consistent with the FN plot of the quasi-one-dimensional model [10]. For the semiconducting tubes, the FN plot has an extra term $-2\gamma\phi^{1/2}/3Fd$, which means that the current decreases exponentially with the diameter of CNs. This is because the energy gap at the Fermi level for the semiconducting tubes is inversely proportional to the diameter of the tubes [14]. In the intermediate region $0.5 < \frac{\gamma\phi^{1/2}}{Fd} < 2$, the I-V characteristic exhibits a more complicate correction to the FN-type behavior. The results in Eqs. (5) and (7) are compared with the FN-type plot $\ln(\frac{j_s(F)}{F^2}) = -\frac{b\phi^{3/2}}{F} + \ln(\frac{\alpha d}{\gamma\phi})$ in Fig. 2. It can be seen that our results agree with the FN behavior for the large-diameter tube [Fig. 2(b)], but the modification to the FN behavior for the small-diameter tube becomes clear in Fig. 2(a), especially for weak fields. The non-FN behavior of the I-V characteristic observed in experiments can be understood as arising from different physical mechanisms. In our opinion, the non-FN behavior should appear in the SDLF region. In fact, most of the emitters investigated in experiments are more complicated than the ones assumed in the theoretical model, such as CN films mixed in the multiwall and single-wall CNs, or open and capped CNs. These complications could affect the I-V characteristic, such as the layer-layer and tube-tube interactions, and the localized states from defects, impurities, and caps. We cannot clarify experimentally which factor dominates the behavior of the I-V characteristic. Thus, it is should not very appropriate to compare directly the theoretical results with the experimental observations.

Interestingly, Gogolin and Komnik studied the Luttinger liquid (LL) model of one-dimensional interacting electrons to give a FN-like formula of emission current [15] $j_{\mathrm{LL}} \propto (\frac{F^2}{\phi})^{1/2g} e^{-b\phi^{3/2}/F}$, where g is the LL parameter. The I-V

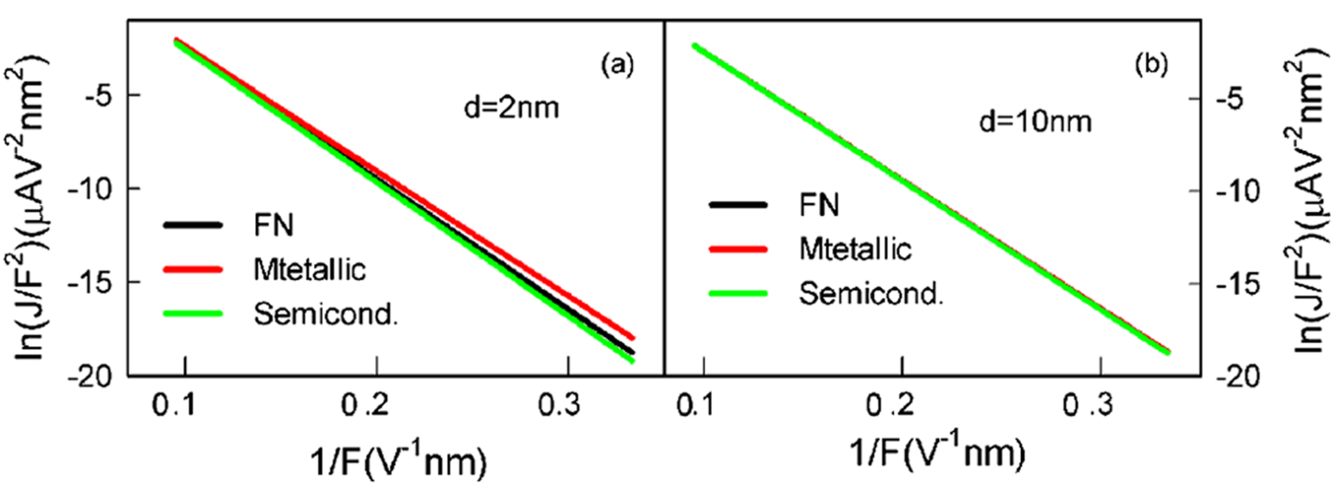

FIG. 2 (color online). The FN plots of the I-V characteristic for the SWCNs with the diameter $d = 2$ nm in (a) and $d = 10$ nm in (b), in which we compare the generalized results in Eqs. (5) and (7) of the metallic and semiconducting SWCNs with the FN-type behavior.

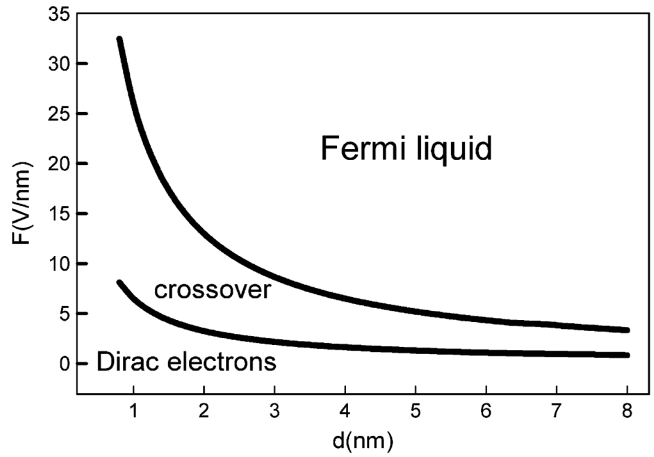

FIG. 3. The phase diagram on the I-V characteristic. The upper region represents the FL behavior, the lower region represents the DE behavior, and the intermediate region is their crossover.

characteristic of the LL emission current depends on the electron-electon interaction. For SWCN, $g = 1/2$, the emission current of the LL reduces to the above FN formula j_{FN}. For the weak interaction limit $g = 1$, the emission current becomes $j_{LL} \propto (F/\sqrt{\phi})e^{-b\phi^{3/2}/F}$, which is consistent with our result for the SDLF case.

The FN-type behavior j_{FN} of conventional metals may be regarded as the Fermi liquid (FL) behavior in field emission. Our generalized FN theory is developed based on the linear energy dispersion of SWCNs with quantization transverse modes. This is a typical characteristic of Dirac electrons. The deviation from the FN behavior in our formalism may be regarded as a Dirac-electron behavior in field emission. Thus, in the SDLF region of metallic tubes $\frac{\gamma\phi^{1/2}}{Fd} > 2$, the I-V characteristic in Eq. (8) corresponds to the Dirac-electron behavior. Thus, we give a phase diagram of the CN field emission in Fig. 3, in which we can observe the Fermi liquid behavior in the upper region, the Dirac-electron behavior in the lower region, and the crossover in the intermediate region.

In summary, taking the energy band structure of SWCNs into account, we develop a generalized FN theory of CNs and obtain the analytic formulas of the I-V characteristics for metallic and semiconducting CNs. This formalism provides a tube diameter versus electric field phase diagram of the I-V characteristic, identifying the modified FN-type behavior (FL) in the LDHF region, the Dirac-electron (DE) behavior in the SDLF region, and their crossover in the intermediate region. Based on this theory, the experimental non-FN-type phenomenon may be regarded as a Dirac-electron behavior in the SDLF region. The field-emission behavior depends on the size of the emitters and the field strength. Actually, the SWCN is a typical quasi-one-dimensional system, which contains some key characteristics of low-dimensional systems. Therefore, this theory may be considered as describing these characteristics of the field emission of low-dimensional systems.

The authors gratefully thank Paul Erdos for his critical reading of the manuscript. This work is supported financially by the National Natural Science Foundation of China (Grants No. 10774194, No. 90306016, No. U0634002, and No. 50572123), National Basic Research Program of China (973 Program: No. 2007CB935501), and Advanced Academic Center of Sun Yat-Sen University (06P4-3).

*Corresponding author.
stslsd@mail.sysu.edu.cn
†Present address: Shanghai Institute of Optics and Fine Mechanics, Chinese Academy of Sciences, Shanghai 201800, People's Republic of China.

[1] J. M. Bonard *et al.*, Solid-State Electron. **45**, 893 (2001); J. M. Bonard *et al.*, Appl. Phys. A **69**, 245 (1999); J. M. Bonard *et al.*, Phys. Rev. Lett. **89**, 197602 (2002).
[2] Niels de Jonge *et al.*, Nature (London) **420**, 393 (2002); Niels de Jonge, J. Appl. Phys. **95**, 673 (2004).
[3] R. H. Fowler and L. W. Nordheirm, Proc. R. Soc. A **119**, 173 (1928); L. W. Nordheirm, Proc. R. Soc. A **121**, 626 (1928); Richard G. Forbes, J. Vac. Sci. Technol. B **17**, 526 (1999).
[4] W. A. de Heer, A. Chatelain, and D. Ugarte, Science **270**, 1179 (1995); W. A. de Heer *et al.*, *ibid.* **268**, 845 (1995); A. G. Rinzler *et al.*, *ibid.* **269**, 1550 (1995).
[5] M. R. Falvo *et al.*, Nature (London) **389**, 582 (1997); J. P. Barbour *et al.*, Phys. Rev. **92**, 45 (1953).
[6] Xiao Zheng *et al.*, Phys. Rev. Lett. **92**, 106803 (2004).
[7] Shi-Dong Liang *et al.*, Appl. Phys. Lett. **85**, 813 (2004); Shi-Dong Liang *et al.*, J. Vac. Sci. Technol. B **24**, 983 (2006).
[8] Marc Bockrath *et al.*, Nature (London) **397**, 598 (1999); Reinhold Egger, Phys. Rev. Lett. **83**, 5547 (1999); L. S. Levitov and A. M. Tsvelik, *ibid.* **90**, 016401 (2003).
[9] A. Modinos, *Field, Thermionic, and Secondary Emission: Emission Spectroscopy* (Plenum Press, New York, 2002).
[10] V. Filip, D. Nicolaescu, and O. Okuyama, J. Vac. Sci. Technol. B **19**, 1016 (2001).
[11] J. W. Mintmire and C. T. White, Phys. Rev. Lett. **81**, 2506 (1998).
[12] Lu Chen, Bachelor thesis, Sun Yat-Sen University, 2006.
[13] J. W. Gadzuk and E. W. Plummer, Rev. Mod. Phys. **45**, 487 (1973).
[14] R. Saito, G. Dresselhaus, and M. S. Dresselhaus, *Physical Properties of Carbon Nanotubes* (Imperial College Press, London, 1998).
[15] Andrei Komnik and Alexander O. Gogolin, Phys. Rev. B **66**, 035407 (2002); Alexander O. Gogolin and Andrei Komnik, Phys. Rev. Lett. **87**, 256806 (2001).